Tellus (2005), 57A, 770–782
Printed in Singapore. All rights reserved

TELLUS

Water vapor budget of the Indian monsoon depression

By JIN-HO YOON and TSING-CHANG CHEN*, *Department of Geological and Atmospheric Sciences, Iowa State University, 3010 Agronomy Hall, Ames, IA 50011, USA*

(Manuscript received 25 July 2004; in final form 18 February 2005)

ABSTRACT

Estimations by previous studies show that a minor amount of the Indian monsoon rainfall is contributed by Indian monsoon depressions (IMDs). In contrast, other studies found that approximately half of the summer monsoon rainfall in the northern Indian subcontinent is generated by IMDs. IMDs occur an average of six times during the summer season and provide a crucial water source to the agricultural activity over this region. The large disparity in the estimation of the IMD contribution to the Indian rainfall by previous studies requires a more accurate water vapor budget analysis of the IMD with quality data. For this reason, a composite analysis of the IMD is performed using the ERA-40 reanalysis and four precipitation data sets (the Global Precipitation Climatology Project, the Tropical Rainfall Measuring Mission, the GEOS precipitation index at the Goddard Space Flight Center and surface station observations) for the period of 1979–2002. Important findings of this study are: (i) about 45–55% of the total Indian rainfall is produced by the IMD; (ii) the rainfall maximum in the west–south-west sector of IMDs is largely maintained by convergence of atmospheric water vapor flux. The convergence of water vapor flux is largely coupled with the lower-tropospheric divergent circulation. Thus, the IMD water vapor budget is modulated by the 30–60 and 10–20 d monsoon modes through changes of water vapor convergence/divergence. The magnitude of this modulation on the IMD water vapor budget is close to a quarter of the summer-mean water vapor budget over the Bay of Bengal and north-eastern India.

1. Introduction

Monsoon rainfall, which is generated by different weather systems including tropical cyclones, weak disturbances, depressions, etc., has a profound impact on human activity in India (Ramage, 1971). Among these weather systems, the Indian monsoon depression (IMD) is the most prolific rain producer/distributor in the Indian summer monsoon system because of its frequent occurrence and generation of a large amount of rainfall. On average, six monsoon depressions are formed every monsoon season (June to August) over the Bay of Bengal (Saha et al., 1981; Chen and Weng, 1999). These depressions migrate deep into the Indian subcontinent and bring a substantial amount of monsoon rainfall along their tracks (e.g. Krishnamurti, 1979). However, due to the lack of quality observations over the ocean, the IMD water vapor budget and the evolution of this budget during different phases of the IMD life cycle have not been well explored. A comprehensive effort along this line was made in this study.

An IMD has a lifespan of about 5 d, a westward phase speed of approximately 6 m s^{-1} (5° longitude d^{-1}) and a wavelength of 2000–2500 km (e.g. Krishnamurti et al., 1975, 1976; Daggupaty and Sikka, 1977). It was observed that the south-west quadrant of a monsoon depression could receive a rainfall of 100–200 mm over a 24-h period (e.g. Daggupaty and Sikka, 1977; Stano et al., 2002). Using six stations (Calcutta, Allahabad, Delhi, Goplur, Nagpur and Ahmadabad), Mooley (1973) estimated that only a minor amount of the total rainfall during the monsoon season is contributed by IMDs. In contrast, it was pointed out by Krishnamurti (1979) and Saha et al. (1981) that IMDs bring India about half of its summer monsoon rainfall. Such a large difference in the estimation of the IMD's contribution to the Indian monsoon rainfall by different studies requires a more accurate analysis of the IMD water vapor budget with quality data.

Due to the limited availability of quality observations over oceans adjacent to India (Bay of Bengal, Arabian Sea and the Indian Ocean), previous studies dealing with IMDs (e.g. Nitta and Masuda, 1981; Saha and Chang, 1983; Saha and Saha, 1988) focused only on the structure and heat budget of a few special cases during a field experiment (e.g. MONEX). The water vapor budget of these IMDs has not been analyzed. It was pointed out by previous studies (e.g. Saha and Saha, 1988) that heavy rainfall associated with an IMD occurred primarily over its south–south-west sector. However, the cause of the rainfall maximum in this quadrant of an IMD and the evolution of this rainfall maximum coupled with the IMD life cycle has not been explored. In order to search for this cause, an extensive analysis of the IMD water vapor budget is needed.

*Corresponding author.
e-mail: tmchen@iastate.edu

The Indian monsoon life cycle (onset–break–revival–withdrawal) is regulated by two intraseasonal modes: the 30–60 and 10–20 d monsoon modes. The maximum (minimum) monsoon rainfall as well as monsoon westerlies, i.e. active (break) phase, occur when the 30–60 d monsoon trough (ridge) arrives at 15°–20°N to deepen (fill) the monsoon trough over northern Indian (Krishnamurti and Subrahmanayam, 1982; Chen and Yen, 1986). On the other hand, the 10–20 d monsoon mode can also modulate the large-scale circulation and monsoon rainfall over the Indian subcontinent (Krishnamurti and Bhalme, 1976; Murakami, 1976). The activity of the westward propagating IMD along the Indian monsoon trough is likely to be affected by the 10–20 d mode. It is conceivable that any change in the large-scale circulation caused by the two intraseasonal modes may exert some impact on the IMD occurrence frequency. Can these two intraseasonal monsoon modes also affect the water vapor budget of the IMD? The modulation of the Indian monsoon life cycle (reflected by the large-scale monsoon circulation and rainfall) by the two intraseasonal modes suggests that the water vapor budget and hydrological processes of an IMD may be modulated by the 30–60 and 10–20 d monsoon modes.

Because of its importance to the Indian monsoon rainfall, the water vapor budget of the IMD becomes a major concern of this study with a focus on the following aspects: (i) the IMD contribution to total monsoon rainfall over India; (ii) the evolution of water vapor budget and hydrological processes of the IMD; (iii) the modulation of the IMD water vapor budget by the 30–60 and 10–20 d monsoon modes. Thus, the present study is arranged in the following way. Data and analysis methods used in this study are presented in Section 2. For reference and comparison, the water vapor budget of the monsoon system and two intraseasonal modes are shown in Section 3, prior to the water vapor budget analysis of the IMD. The water vapor budget and hydrological processes of the IMD are displayed in Section 4. The modulation of the IMD water vapor budget by the two intraseasonal modes is discussed in Section 5, and concluding remarks are offered in Section 6.

2. Data and analysis methods

2.1. Data

Analyses of the IMD water vapor budget and hydrological processes involved in this budget were performed in this study with two different data sources: observed precipitation and reanalyses. Because of the lack of rainfall observations over oceans, satellite observations become an indispensable alternative. Three different types of precipitation generated with satellite observations were used in this study: (1) direct rainfall measurements by satellite through the Tropical Rainfall Measuring Mission (TRMM; Simpson et al., 1996); (2) GEOS precipitation index (GPI) generated with satellite infrared (IR) observations at the Goddard Space Flight Center (Susskind et al., 1997); (3) rainfall compiled through the Global Precipitation Climatology Project (GPCP; Huffman et al., 1997) by merging rain-gage measurements and rainfall proxies generated with satellite data. Based on satellite IR observations, daily GPI with a $1^\circ \times 1^\circ$ horizontal resolution were available for the 1979–97 period. For the period from 1998 to 2002, daily rainfall is furnished by the GPCP and the TRMM. The GPCP rainfall was produced by a merged analysis incorporating precipitation from low-orbit-satellite microwave observations, geo-synchronous satellite IR data, and rain-gage measurements with a $1^\circ \times 1^\circ$ horizontal resolution. The TRMM daily rainfall (3B42 obtained from http://lake.nascom.nasa.gov) is created by combining the TRMM estimates with the different satellite estimations (including the gridded SSM/I estimates) and rain-gage observations. After 1997, the ensemble average of both the TRMM and GPCP daily rainfall was used in our analysis.

Heavy rainfall over land may not be properly represented by the GPI. To make the quality of estimated rainfall more uniform over both land and oceans, the GPI was blended with station reported rainfall compiled by the Climate Prediction Center (CPC; DS512.0, CPC global summary of day/month observations from 1979 to current days). The CPC station rainfall data include approximately 8900 observations of actively reporting stations around the world. In our analysis, all available station data were used. Maximum station numbers covered by our analysis domain (including Indochina and some part of China) reach 1000. However, this blending procedure was applied only to the GPI because the GPCP and the TRMM rainfall estimations already included rain-gage observations. The merger of two rainfall data sets was accomplished using the following steps. Station rainfall data were interpolated by the Cressman scheme[1] (Cressman, 1959) onto the $1^\circ \times 1^\circ$ grid, and then merged with the GPI. Weighting factors were also incorporated into the merging procedure: a factor of 0.7 was applied to the station data over land, and a factor of 0.3 was applied to the GPI. On the other hand, the GPI weighting was increased toward the oceans to reduce a sudden change of rainfall across the boundary. In addition to the GPI, outgoing long-wave radiation (OLR) observed by the polar orbital satellites of the National Oceanic and Atmospheric Administration (NOAA; obtained from the Climate Diagnostic Center, NOAA) was also used as an indicator of deep convection in the tropics and subtropics during summer to gage the quality of rainfall represented by the GPI.

Other meteorological variables (e.g. wind field and specific humidity) were obtained from the European Centre for

[1]The radius of influence in the Cressman scheme used in the analysis of station rainfall is 2° (~200 km). The weighting factor (W) with the radius of influence (R) is $W = 1 - (r/R)^2$, where r is the distance of observational location from a given grid point. With this weighting factor, the major contribution of station observations comes from stations within the radius of 1° (where $W = 0.75$, but drops dramatically outside this radius).

Medium-Range Weather Forecasts (ECMWF) reanalysis data (Gibson et al., 1997) for the 1979–2002 period. In this study, our analysis used only the ECMWF reanalyses at 00 and 12 UTC because rawinsonde observations were available at these synoptic times.

2.2. Analysis methods

The water vapor budget of monsoon depression was analyzed with the following budget equation

$$\frac{\partial W}{\partial t} + \nabla \cdot Q = E - P, \tag{1}$$

where W, Q, E and P are precipitable water, the vertically integrated water vapor flux, evaporation and precipitation, respectively. Individual terms in eq. (1) are computed by the following procedure. The storage term ($\partial W/\partial t$) is computed in terms of the centered finite difference scheme with a time interval of 12 h. Because of the lack of observations, evaporation is estimated by the residual method

$$E = \frac{\partial W}{\partial t} + \nabla \cdot Q_{\mathrm{D}} + P,$$

which may include bias of the data assimilation system and computation error. Following Chen (1985), divergent components of water vapor flux (Q_{D}) were computed in terms of horizontal gradients of the water vapor flux potential function (χ_Q). χ_Q is obtained by solving $\nabla^2 \chi_Q = \nabla \cdot Q$ in terms of the spectral method based on a horizontal resolution of T63. The regional water vapor budget around the IMD is presented by area-averaged values ($[\ ] = \iint_A \mathrm{d}a$) of individual terms in eq. (1) with a 10° × 10° box centered at the core of the IMD, which can cover the heavy rainfall region of the IMD. Although a typical horizontal scale of an IMD is about 2000–2500 km (e.g. Godbole, 1977; Sikka, 1977), a strong positive vortex in a relatively limited region (≈1000 km) is typical among IMDs (Krishnamurti et al., 1975, 1976).

Krishnamurti et al. (1977) used surface pressure to trace the westward propagation of residual lows across Indochina into the Bay of Bengal, while Saha et al. (1981) applied sea-level isallobaric (24-h surface pressure tendency) to determine the westward-propagating disturbances. Later, Chen and Weng (1999) expanded this IMD identification scheme but primarily focused on the following 850-mb synoptic charts: the 850-mb streamline charts of total, 12–24 d, and 2–7 d filtered winds superimposed with the corresponding unfiltered/filtered OLR, and the 24-h surface pressure tendency charts. Following Saha et al. (1981) and Chen and Weng (1999), the following classification of synoptic perturbations in terms of wind speed is used to define the IMD: low (<8.5 m s^{-1}), depression (8.5–13.5 m s^{-1}), deep depression (14–16.5 m s^{-1}) and cyclonic storm (17–23.5 m s^{-1}). The identification scheme and the definition of the IMD introduced by precious studies, particularly Chen and Weng (1999), are adopted by this study. Tracks of IMDs identified for 1979–1994 were expanded to 2002. In total, there were 143 monsoon depressions identified over 24 summers (1979–2002). Occurrence dates of these cases are shown in Fig. 1.

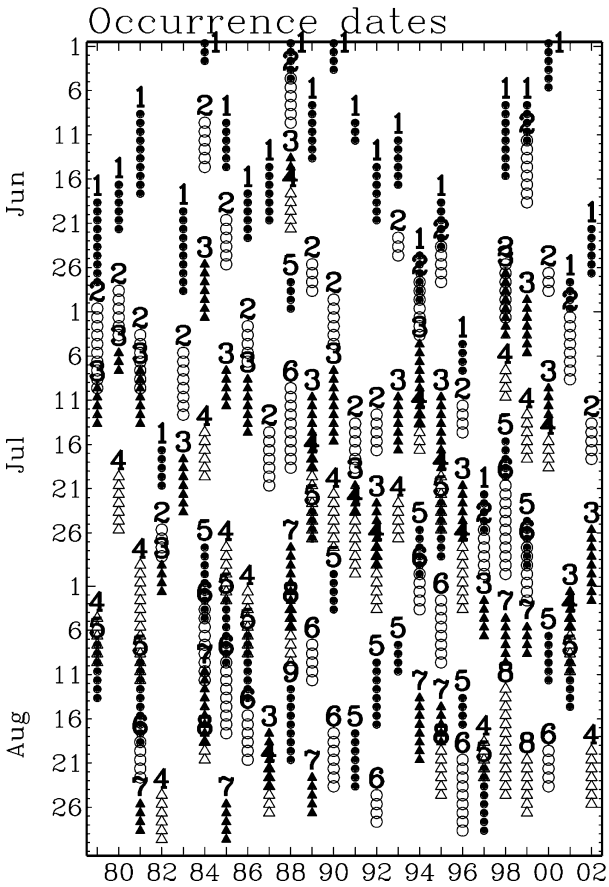

Fig. 1. Occurrence dates of all identified Indian monsoon depressions (143 cases) for 24 summers (1979–2002). Different numerals and symbols are used in the same summer to distinguish one IMD case from the next one.

After its formation in the Bay of Bengal, an IMD migrates westward into the Indian subcontinent with a phase speed about 5° longitude d^{-1}. The distance between Bengadish (∼95°E) and north-west India (∼70°E) covers 25° longitude. On average, it takes about 5 d for an IMD to propagate through the Indian subcontinent. Coincidentally, the average life cycle of an IMD is about 5 d. In other words, an IMD dissipates after it propagates through the Indian subcontinent. To illustrate the time evolution of an IMD, a composite scheme was developed in terms of its averaged westward propagation speed. First, the average location of all IMDs within a 5° longitudinal zone is obtained and the centers of all IMDs within this longitudinal zone are adjusted to match this averaged center. For example, all IMDs with centers located between 95°E and 90°E are averaged to form the IMD center for day 1. Thus, the composite IMD life cycle spans 5 d (days 1 to 5) after it is formed. Before the system reaches the Bay of Bengal, it is classified as the 'prior depression phase'

(equivalent to the residual low). Two days (days $-2 \sim -1$) before the formation of an IMD will be used to illustrate this phase. After reaching the Bay of Bengal, the depression with its rainfall larger than 25 mm d^{-1} is identified as phase 2 (days 2–4). The 5-d lifespan of an IMD is based upon its average phase speed. However, some IMDs with a phase speed slower/faster than 5° longitude d^{-1} (Fig. 1) may exist. Phases of these IMDs are still decided by their longitudinal location. The evolutions of monsoon depressions prior to and post phase 2 are classified as phase 1 (day 1) and phase 3 (day 5), respectively, when the system exhibits development (decaying) over the Bay of Bengal (the west coast of India).

The life cycle of an IMD is illustrated in terms of composite charts of different variables during different phases of this depression. This composite procedure enables us to obtain a clear perspective of the IMD's evolution and the water vapor budget/hydrological processes over its life cycle. The maximum horizontal scale of the IMD is about 3000 km (waves 12–13 at 20°N). Therefore, a Fourier spectral filter is used to isolate the short-wave regime (denoted as $[\,]^S$) of waves 6–25 in such a way that the IMD hydrological processes can be well illustrated in comparison with the IMD dynamical processes presented by Chen and Yoon (2000).

The intraseasonal oscillation (30–60 and 10–20 d) signals of a variable were isolated using the Butterworth bandpass filter (Murakami, 1979). The filtered rainfall over our analysis domain (75°E–90°E, 15°N–27°N) and the zonal wind at the location of (65°E, 15°N) in the Arabian Sea are used as monsoon indices to determine the monsoon life cycles. These cycles were determined by a threshold of 0.8 (-0.8) standard deviations of these two indices. In other words, when monsoon rainfall and westerlies are larger (smaller) than 0.8 standard deviation of the summer-mean values, the monsoon condition is defined as the active/maximum (break/minimum) phases of the 30–60/10–20 d monsoon modes, respectively.

3. Water vapor budget of the Indian summer monsoon

The Indian summer monsoon rainfall undergoes a life cycle modulated by the 30–60 and 10–20 d monsoon modes. Therefore, before the detailed analysis of the IMD water vapor budget is discussed, the water vapor budget of the Indian monsoon and its modulation by these two intraseasonal modes are presented in this section as background.

3.1. Summer climatology

The summer (JJA) hydrological process of the Indian monsoon is depicted with the long-term summer-mean potential function of water vapor flux, divergent water vapor flux and rainfall (χ_Q, Q_D, P) in Fig. 2a. The summer monsoon resides within the convergent cell of the global water vapor flux, which has a major rainfall center in the western tropical Pacific (Chen, 1985). Over the Indian monsoon region, water vapor flux converges toward the monsoon trough to maintain monsoon rainfall centered over the head Bay of Bengal, and north-east and the western coast of India (Fig. 2a). Quantitatively, the regional water budget measured over the computational domain (75°E–90°E, 15°N–27°N, covering part of the Bay of Bengal, and north-east India, as indicated by thick solid line in Fig. 2a) is shown in Fig. 3a. The analysis domain, which is close to that used by Goswami et al. (1999), was selected in order to cover the majority of monsoon depression tracks. The area-averaged rainfall $[P]$ is about 12 mm d^{-1} and the convergence of water vapor flux $[\nabla \cdot Q]$ is approximately 7 mm d^{-1}, which accounts for about 60% of rainfall. Although, the computational domain covers only a part of the Bay of Bengal, evaporation $[E]$ still contributes up to 40% of the total rainfall amount (e.g. Saha and Bavardeckar, 1976). Regardless of the contribution of evaporation to the water vapor budget over the designated domain, rainfall is largely maintained by the convergence of water vapor flux.

3.2. The 30–60 d monsoon mode

The Indian summer monsoon is primarily developed by the seasonal change of the atmospheric circulation in response to the annual variation of diabatic heating. If the annual march of the solar heating is the only forcing, the evolution of the Indian monsoon should follow a periodical annual cycle. Actually, the northward migration of the 30–60 d monsoon trough/ridge (Krishnamurti and Subrahmanayam, 1982), which is linked to the global eastward propagation of the 30–60 d mode (e.g. Chen et al., 1988), modulates the Indian monsoon to form its life cycle (onset–break–revival–withdrawal). During an active phase, the monsoon trough deepens as monsoon westerlies, the convergence of water vapor flux and monsoon rainfall are intensified. In contrast, intensities of the monsoon circulation and hydrological processes are weakened during a break phase. Monsoon rainfall over the Indian subcontinent was often used as a monsoon index, while the zonal wind index over the Arabian Sea was also proposed by Krishnamurti and Subrahmanayam (1982) to define the Indian monsoon life cycle. In the present study, both the 30–60 d filtered rainfall $[\tilde{P}]$ over the computational domain shown in Fig. 2a and zonal wind $\tilde{U}$(850 mb) at (65°E, 15°N) of the Arabian Sea were employed to indicate the monsoon life cycle. The role played by this 30–60 d monsoon mode is illustrated in terms of the contrast of horizontal charts of filtered streamline at 850 mb superimposed with filtered rainfall between active and break phases. Composite charts of active/break phases ($\tilde{\chi}_Q$, $\tilde{Q}_D$, $\tilde{P}$) and the area-averaged water vapor budget ($[\nabla \cdot \tilde{Q}_D]$, $[\tilde{P}]$) are presented in Figs. 3b–c and 2b–c. Salient features of the water vapor budget and hydrological process during the active/break monsoons are summarized as follows.

(i) The active (break) phase of the Indian monsoon is characterized by convergence (divergence) anomalies of water vapor flux and more (less) rainfall in the northern part of India

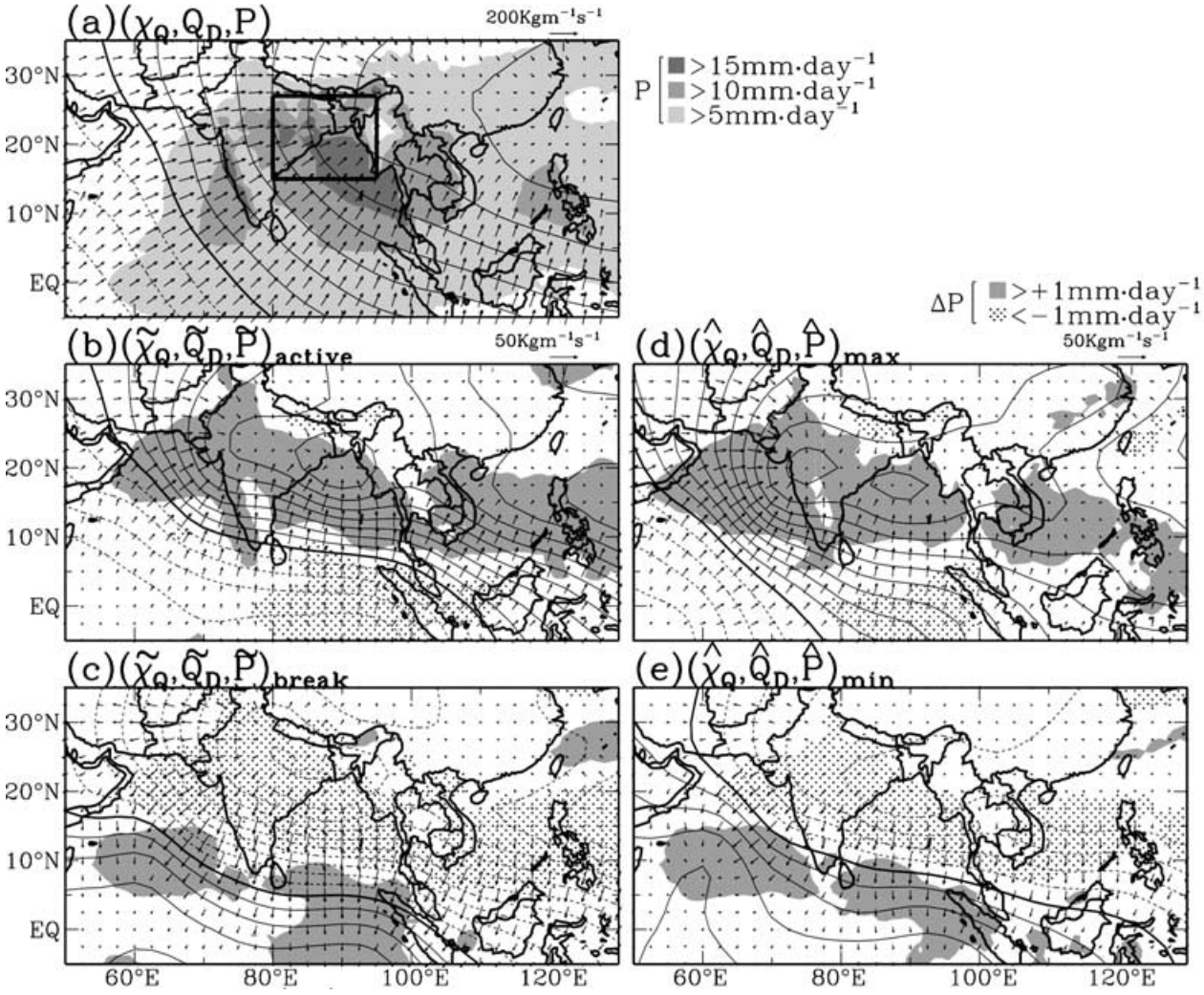

Fig. 2. (a) Summer-mean potential function of water vapor flux (χ_Q), the divergent water vapor flux (Q_D), and precipitation (P). (b) ($\tilde{\chi}_Q$, $\tilde{Q}_D$, $\tilde{P}$)$_{active}$, (c) ($\tilde{\chi}_Q$, $\tilde{Q}_D$, $\tilde{P}$)$_{break}$, (d) ($\hat{\chi}_Q$, $\hat{Q}_D$, $\hat{P}$)$_{max}$ and (e) ($\hat{\chi}_Q$, $\hat{Q}_D$, $\hat{P}$)$_{min}$, where ($\tilde{}$) and ($\hat{}$) are the 30–60 and 10–20 d filtered ( ) anomalies, respectively. The active and break phases of the 30–60 d monsoon mode and the maximum and minimum phases of the 10–20 d monsoon mode are denoted by ( )$_{active}$, ( )$_{break}$, ( )$_{max}$ and ( )$_{min}$, respectively. Contour intervals are 2×10^9 m^2 s^{-1} g kg^{-1} for (a) and 2×10^8 m^2 s^{-1} g kg^{-1} for (b)–(e), respectively.

(Figs. 2b and c), which are consistent with observations of Murakami et al. (1984) and Cadet and Greco (1987).

(ii) Compared to the long-term summer mean values, the area-averaged water budget during the active/break phases (Figs. 3b and d) exhibits a 25% (about 3 mm d^{-1}) increase (decrease), but evaporation, which is derived from the residual method, reveals no significant change.

3.3. The 10–20 d monsoon mode

Although the life cycle of the Indian monsoon is largely determined by the northward migration of the 30–60 d trough/ridge, the 10–20 d mode can still modulate the monsoon life cycle. Krishnamurti et al. (1984) suggested that the onset of the 1979 summer monsoon was caused by a phase lock of the 30–60 and the 10–20 d modes. The synoptic structure and the role of the 10–20 d monsoon mode in the Indian monsoon life cycle have been documented by previous studies (e.g. Murakami, 1976; Krishnamurti and Ardanuy, 1980; Chen and Chen, 1993). However, the impact exerted by this monsoon mode on the regional water vapor budget has not been explored. The approach used to illustrate the impact of the 30–60 d mode on the monsoon water vapor budget is adopted here to deal with the impact of the 10–20 d mode. Composite charts of ($\hat{\chi}_Q$, $\hat{Q}_D$, $\hat{P}$) generated by this approach and the area-averaged water budget ([$\nabla \cdot \hat{Q}_D$], [$\hat{P}$]) are shown in Figs. 2d–e and 3d–e, respectively. Their salient features may be summarized as follows.

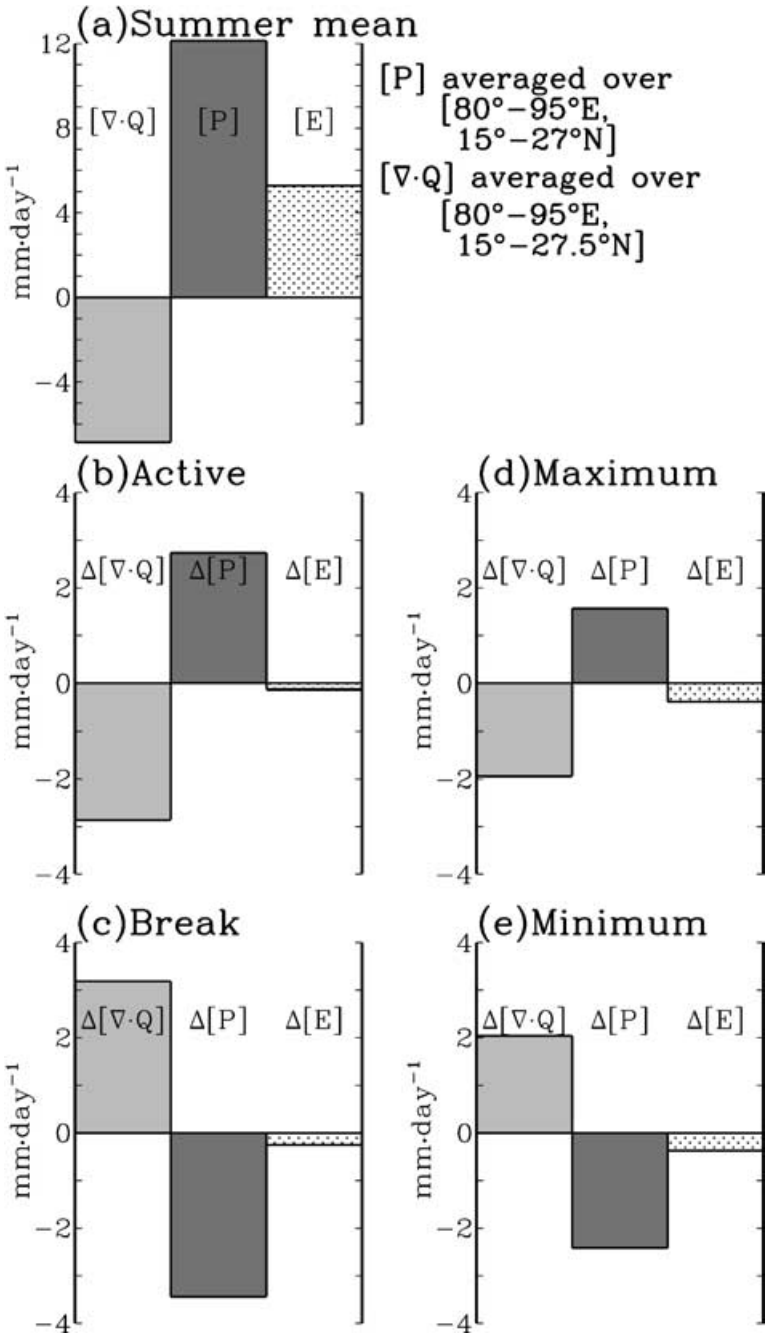

Fig. 3. (a) The summer water vapor budget averaged over the analysis domain (thick-line box in Fig. 2a) and departures of the area-mean water vapor budget from its summer-mean value during phases of (b) active monsoon, (c) monsoon break, (d) 10–20 d maximum and (e) 10–20 d minimum.

(i) The 10–20 d mode exhibits a dipole structure with a northern cell at about 20°N and an equatorial cell (Chen and Chen, 1993). The former significantly affects the Indian monsoon rainfall. It is revealed from Fig. 2d (e) that convergence of water vapor flux over India is enhanced (suppressed) during the maximum (minimum) phase.

(ii) Compared to the long-term summer mean, rainfall and convergence of water vapor flux are increased (decreased) about 17% by the 10–20 d mode during maximum (minimum) phases. The effect of the 10–20 d mode on the monsoon water budget over the analysis domain of Fig. 2a is slightly smaller than that of the 30–60 d mode.

4. Water budget of the Indian monsoon depression

The westward propagating IMD is a major rainfall producer in the Indian subcontinent, but its water vapor budget and

hydrological processes have not been extensively analyzed. For this reason, the following questions are raised: (i) how much of the Indian monsoon rainfall is contributed by IMDs and (ii) what is the major hydrological process of IMD to generate associated rainfall? These questions will be answered in terms of composite charts of different hydrological variables in four phases of the IMD life cycle (prior depression, initial, mature and decay). The 850-mb monsoon flow embedded with an IMD and the water vapor budget of this depression during its different phases are shown in Figs. 4 and 5, respectively. Let us highlight major features of the IMD circulation structure and water vapor budget of particular interest to this study.

(i) Prior depression phase (residual low from day −2 to day −1). The westward propagation of the residual low across Indochina is clearly shown in the 850-mb streamline chart superimposed with the short-wave streamfunction anomalies (shading areas) in Fig. 4a, consistent with observations of Saha et al. (1981) and Chen and Weng (1999). Less-organized rainfall at this stage (Fig. 4b) is maintained by weak convergence of water vapor flux east of the system.

(ii) Phase I (formation of monsoon depression over the Bay of Bengal at day 1). After reaching the Bay of Bengal, the residual low develops into an IMD. Flow of the depression is strengthened at this time. The convergence of water vapor flux and rainfall indicated by $(\Delta\chi_Q^{\mathrm{S}}, \Delta Q_{\mathrm{D}}^{\mathrm{S}}, P)^{\mathrm{C}}$ form a well-organized center west/south-west of the depression. The spatial relationship between the rainfall center and the newly developed depression center is opposite to that during the prior depression phase (Fig. 4b).

(iii) Phase 2 (mature during days 2–4). During this phase, the IMD moves westward from the head Bay of Bengal to northwestern India. As it propagates into the subcontinent, the depression brings a large amount of precipitation into India. The major moisture source of the IMD at this stage is the convergence of water vapor flux instead of evaporation. This argument will be substantiated later (Fig. 5a). On day 4, convergence of water vapor flux starts to weaken (Fig. 5a). Over the entire phase 2, the enhancement (reduction) of the depression rainfall is primarily attributed to convergence (divergence) of water vapor flux.

(iv) Phase 3 (decay at day 5). A depression may still maintain its circular/symmetric flow in the lower troposphere, but the reduction of water vapor supply by the convergence of water vapor flux ($\approx$9 mm d^{-1}) leads to the depression's decay. The water vapor budget of an IMD during this phase is characterized by a drastic reduction in the water vapor supply by the water vapor flux convergence.

The most interesting finding obtained from composite charts of the 850-mb streamline and hydrological process in company with the IMD development (Fig. 4) is the spatial relationship between the low center of a disturbance and major rainfall prior to and after the IMD formation over the Bay of Bengal. Rainfall was located east of the low center during the prior IMD phase, but this spatial relationship is reversed after the IMD formation phase. Based on the thermal advection of a prior FGGE monsoon depression, Saha and Chang (1983) suggested that an asymmetric circulation across an IMD might be formed by the warm (cold) air advection ahead (behind) this depression. It is inferred from the $(\Delta\chi_Q^{\mathrm{S}}, P)^{\mathrm{C}}$ distributions shown in Fig. 4 that this asymmetric circulation should be maintained by the latent heat released from the IMD's rainfall, as argued by Saha and Saha (1988). Evidently, this maintenance mechanism of the IMD asymmetric circulation, which is linked with the IMD's westward propagation (Chen et al., 2005), differs from that of Saha and Chang.

In order to obtain a quantitative measurement of hydrological processes involved with the IMD development (Fig. 4), the composite water budget of IMDs during different phases of its life cycle is shown in Fig. 5a. The water vapor storage term $(\partial W/\partial t)$ is generally negligible over the entire life cycle of the IMD. Precipitation and the convergence of water vapor flux reach their maximum at day 2, but the variation in the intensity of the hydrological cycle of the IMD is relatively steady even when the system moves inland. On the last day (day 5), despite the non-negligible evaporation, convergence of water vapor flux is reduced to about half of day 2 maximum. This drop in convergence of water vapor flux at day 5 may be contributed by a planetary-scale factor: the IMD is close to the boundary between the positive and negative global χ_Q cell (Fig. 2a). Based on the comparison of magnitude, the water vapor budget shown in Fig. 5a indicates that the major water vapor supply of IMD rainfall is convergence of water vapor flux, instead of evaporation. For tropical storms, water vapor is mainly supplied by the evaporation from the warm ocean surface (Riehl, 1954) so that the storm's intensity is rapidly reduced after landfall. The maintenance mechanism of an IMD's water vapor budget is similar to mid-latitude cyclones (Chen et al., 1996) in the sense that rainfall is primarily maintained by convergence of water vapor flux.

The importance of the IMD contribution to the Indian summer monsoon rainfall may be assessed by how much rainfall is produced by IMDs in comparison with those contributed by 30–60 and 10–20 d monsoon modes and summer-mean rainfall of the Indian monsoon averaged over the analysis domain shown in Fig. 2a. The amounts of rainfall and convergence of water vapor flux averaged over the IMD life cycle (last histogram in Fig. 5a) are compared with the summer-mean water vapor budget (histogram 1 in Fig. 5b) and the water vapor budget of the two intraseasonal modes during their extreme phases (histograms marked 2 and 3 in Fig. 5b). The average rainfall (convergence of water vapor flux) of the IMD is about two (three) times the summer-mean values and the two intraseasonal monsoon modes during both their active and maximum phases. This contrast shows clearly that the IMD is an effective producer/distributor of monsoon rainfall over the Indian subcontinent.

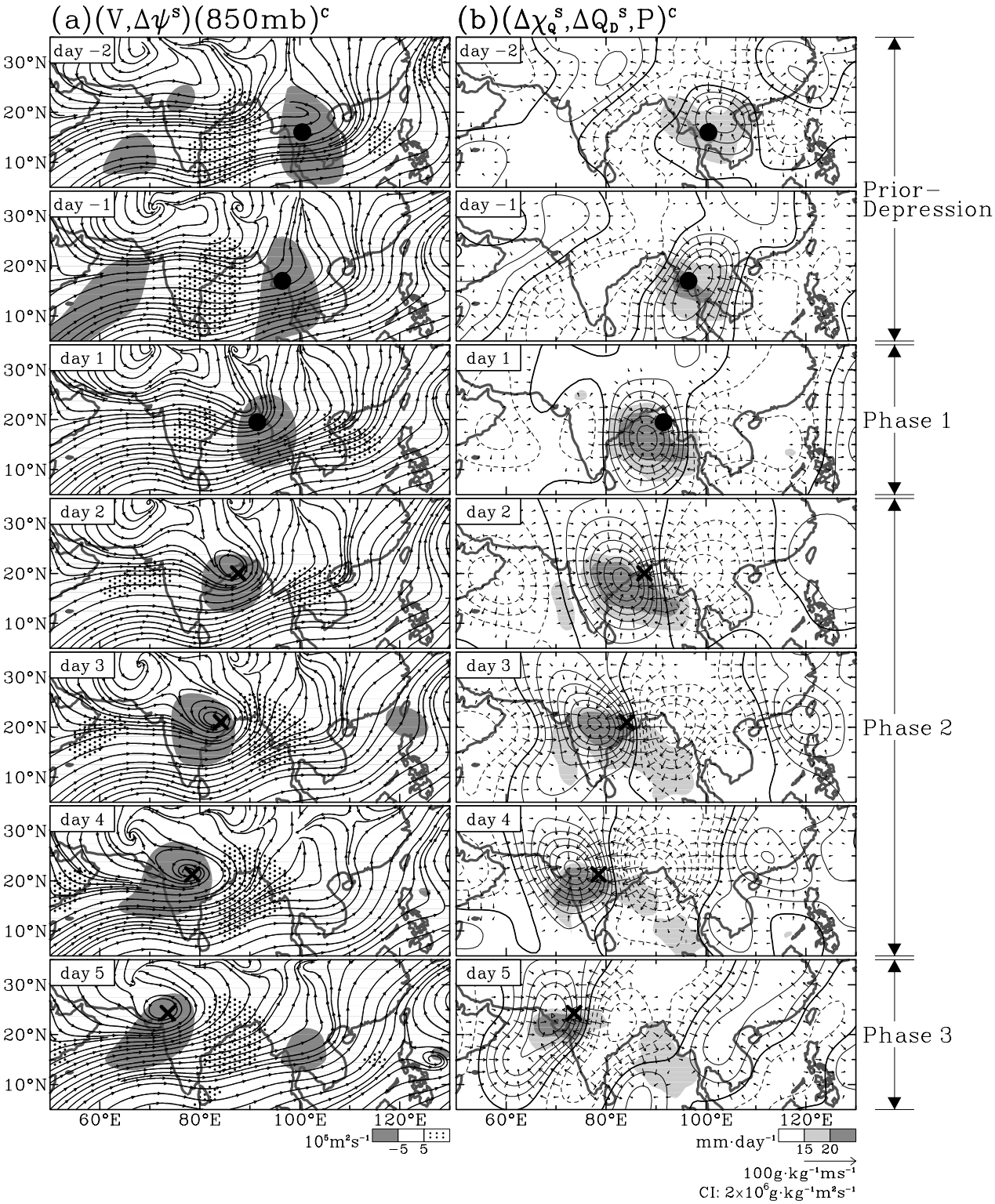

Fig. 4. A composite of monsoon depression during 24 summers (1979–2002) for 7 d [5 (2) days after (before) formation of the monsoon depression] using (a) wind at 850 mb superimposed with departures of the short-wave streamfunction at 850 mb (waves 6–25) [$(V, \Delta\psi^{S})$ (850 mb)^{C}] and (b) departures of the potential function and the divergent water vapor flux and rainfall [$(\Delta\chi_{Q}^{S}, \Delta Q_{D}^{S}, P)^{C}$]. Contour interval is 2×10^{8} m^{2} s^{-1} g kg^{-1}. $\Delta(\,)$ is departure from the summer-mean value of ( ).

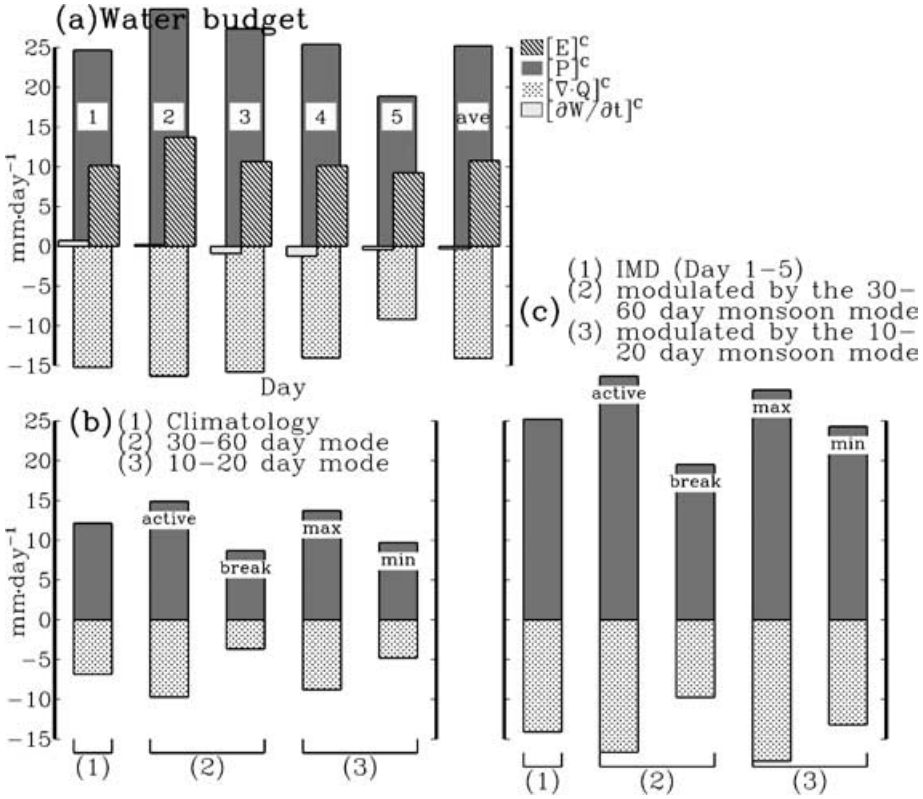

Fig. 5. (a) The composite water vapor budget averaged over 10° longitude × 10° latitude box around the IMD center for this depression's entire life cycle from day 1 to day 5, and its average values (days 1–5). (b) A comparison of the area-averaged rainfall and the divergence of the water vapor flux for long-term summer mean in (1), the 30–60 d monsoon mode in (2), and the 10–20 d monsoon mode in (3). (c) Same as (b) except for the average of all identified IMDs in (1), the composite of the IMD during active/break phases of the 30–60 d mode in (2), and maximum/minimum phases of the 10–20 d mode in (3).

5. Modulation of the water budget of the IMD by the two intraseasonal monsoon modes

The Indian monsoon life cycle is modulated by two intraseasonal (the 30–60 and 10–20 d) monsoon modes. During the active (break) phase of the 30–60 d mode, water vapor converges (diverges) toward (out of) the 30–60 d monsoon trough and enhances (suppress) precipitation (Figs. 2b and c). As shown in Fig. 5b, the water vapor budget analysis of these intraseasonal modes over the domain shown in Fig. 2a reveals that differences in both the convergence of water vapor flux ($-\Delta[\nabla \cdot \tilde{Q}_D]$) and the precipitation ($\Delta[\tilde{P}]$) between active and break phases are about 50% of the climatological values of these two hydrological processes. On the other hand, the 10–20 d mode exhibits a similar, but weaker, impact on the water vapor budget and hydrological processes of the Indian monsoon (about 40% difference between the maximum and minimum phases). Because the major water vapor supply to an IMD is convergence of water vapor flux, it is likely that any change in the convergence of water vapor flux associated with the two intraseasonal monsoon modes may affect the water vapor budget of the IMD.

5.1. Modulation by the 30–60 d mode

The regional water vapor budget of the Indian summer monsoon is profoundly affected by the 30–60 d monsoon mode. The modulation of monsoon rainfall by this intraseasonal monsoon mode may be achieved through the convergence/divergence of water vapor flux associated with the eastward-propagating global divergent circulation (e.g. Chen et al., 1988). To illustrate the possible effect of the 30–60 d monsoon mode on the IMD water vapor budget, we grouped IMDs into two categories: one for the active phase, and another for the break phase. First, the water vapor budgets of all identified IMDs were formed for these two phases of the Indian monsoon life cycle. We then randomly select two IMDs (August 7–9, 1979 and July 6–8, 1996) to illustrate synoptically how the 30–60 d mode affects the IMD water vapor budget. The two phases [phase 1 (formation) and phase 2 (mature)] of the two selected IMDs are shown in Fig. 6.

The IMD during the active phase (August 7–9, 1979) exhibits a street of well-organized cyclonic cells along the monsoon trough. In contrast, the case during the break phase (July 6–8, 1996) shows reduced rainfall and relatively weaker and less-organized cyclonic cell circulation. This contrast is revealed from a comparison between these two IMD cases in Fig. 6a. When

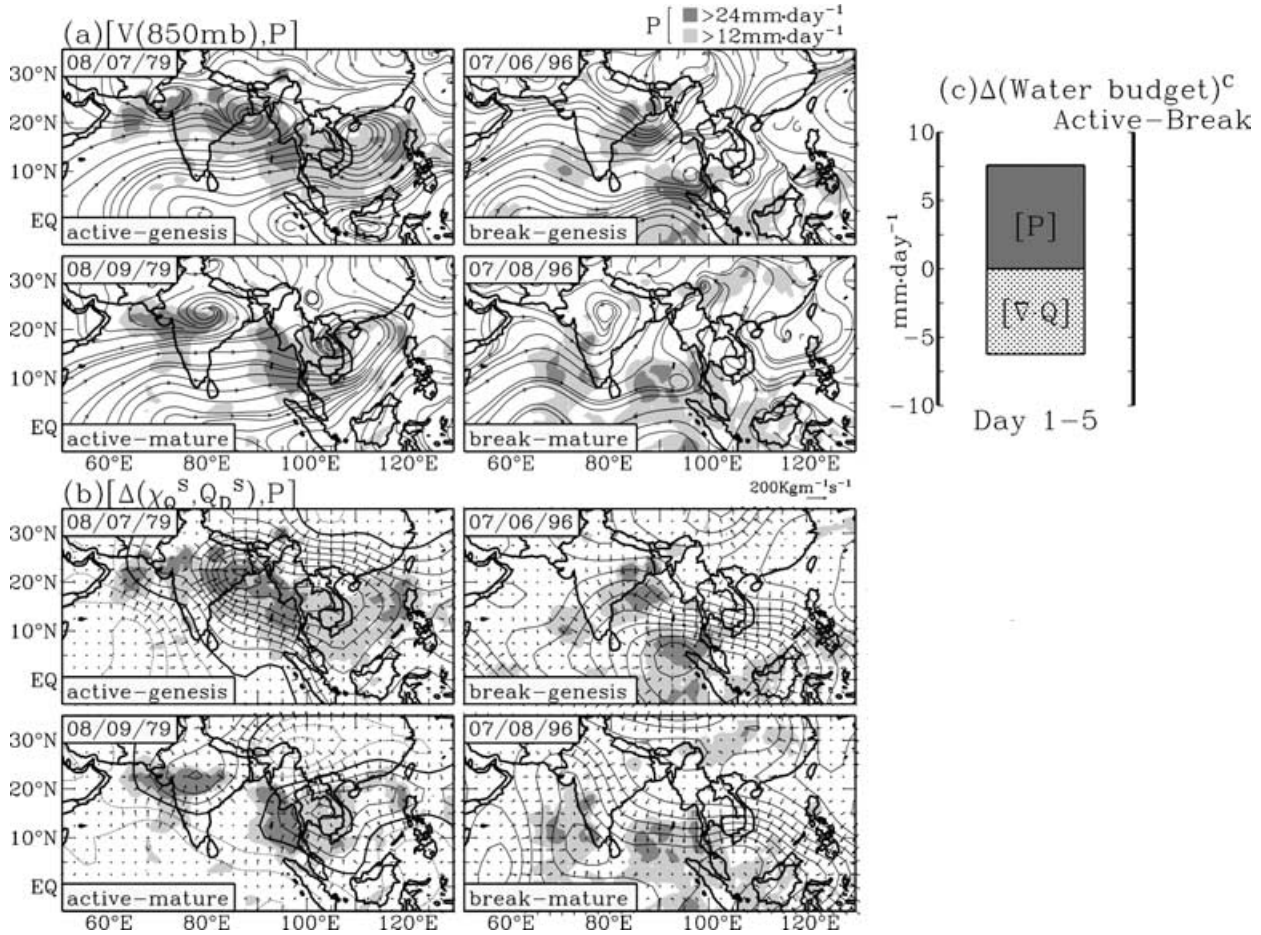

Fig. 6. (a) The 850-mb streamline charts superimposed with P, and (b) the $[\Delta(\chi_Q, Q_D), P]$ field for the IMD cases during the active (August 7–9, 1979) and the break (July 6–8, 1996) phases of the 30–60 d mode, and (c) difference of the IMD water vapor budget between the active and break phases. Each extreme phase of the monsoon cycle includes two days. The IMD formation is portrayed on the first day, while the mature phase is depicted on the second day. The contour interval of $\Delta(\chi_Q)$ is 2×10^8 m^2 s^{-1} g kg^{-1}, where $\Delta(\,)$ is departure from the summer mean.

an IMD reached north-central India (August 9, 1979 and July 8, 1996), it maintained strong (weak) cyclonic circulation with rainfall south-west of its center. Increased (decreased) rainfall of the IMD during the active (break) monsoon phase was maintained by anomalous convergence (divergence) of water vapor flux (Fig. 6b).

The rainfall of the selected IMD during the active monsoon phase is about 40% (compared to the composite IMD rainfall shown in Fig. 5c) more than that during the break monsoon phase. The rainfall increase of the IMD affected by the 30–60 d mode is accompanied by an increase in the convergence of water vapor flux (Fig. 5c). It was shown by Chen and Weng (1999) that the IMD occurrence frequency varies coherently with the 30–60 d monsoon mode. Despite the lower occurrence frequency (Chen and Weng, 1999) and the smaller rainfall of the IMD during the break monsoon phase, the contrast of rainfall and convergence of water vapor flux between the two extreme phases of the Indian monsoon gives us a clear indication of the 30–60 d monsoon mode effect on the IMD hydrological cycle. It becomes clear that the effect of the 30–60 d monsoon mode on the water vapor budget and hydrological process of IMD is accomplished through convergence of water vapor flux. Because the IMD is embedded in the large-scale circulation over India, the effect of the 30–60 d monsoon mode on the Indian monsoon rainfall can be realized through the effect of this intraseasonal monsoon mode on the IMD hydrological cycle.

5.2. *Modulation by the 10–20 d mode*

The procedure used to explore the impact of the 30–60 d mode on the IMD water vapor budget is adopted here to examine the impact of the 10–20 d monsoon mode. Two IMD cases (June 23–25, 1979 and July 22–24, 1991) during the maximum and minimum phases of the 10–20 d mode were selected to illustrate how this mode affects the circulation structure and the water vapor budget of the IMD (Fig. 7).

The IMD (June 23–25, 1979) existed simultaneously with the 10–20 d monsoon low (Fig. 7a), as observed in Chen and

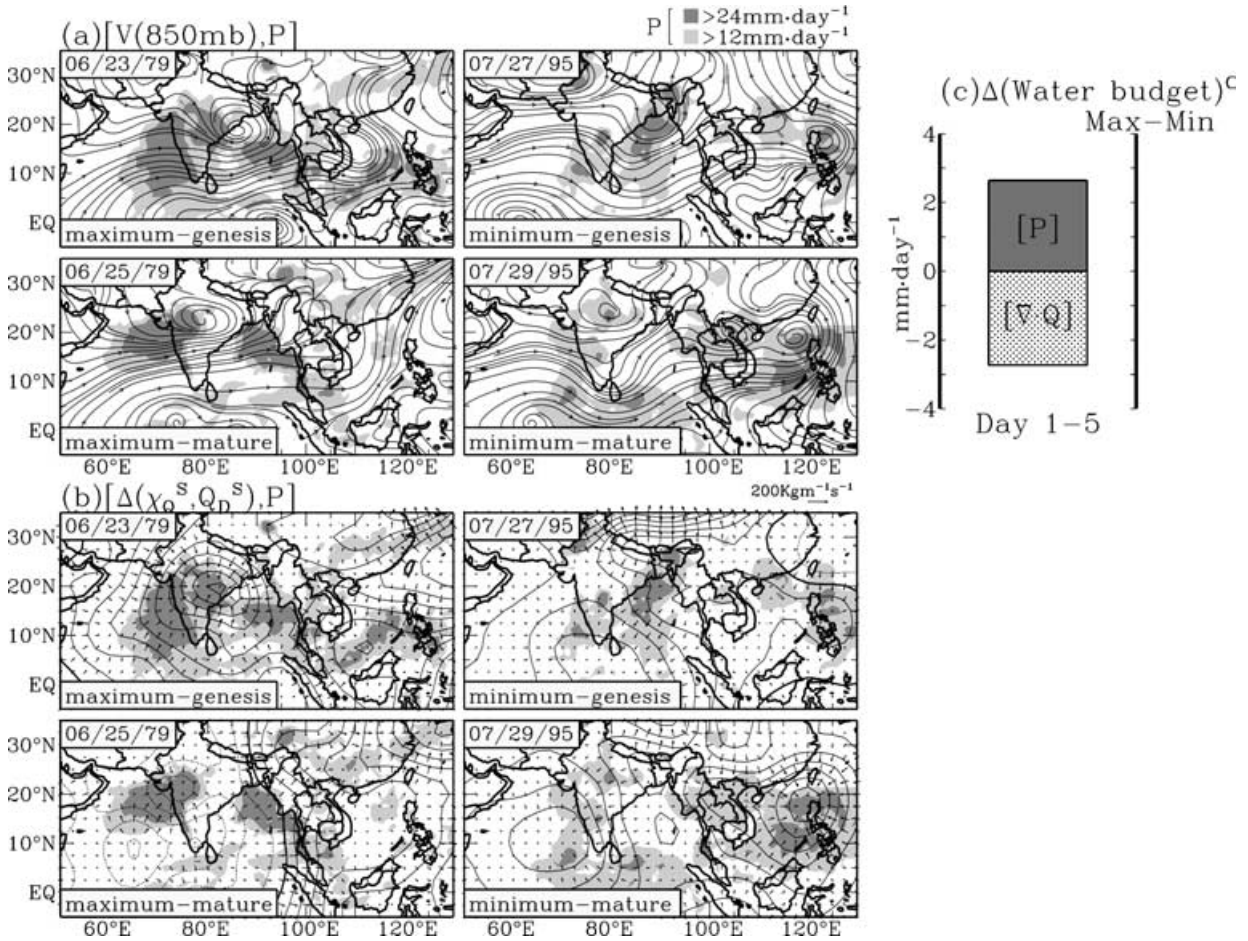

Fig. 7. Same as Fig. 6 except for the maximum (June 23–25, 1979) and minimum (July 22–24, 1991) phases of the 10–20 d monsoon mode.

Chen (1993). It was demonstrated that the intensity of the Indian monsoon low could be strengthened by the 10–20 d monsoon low. Thus, stronger cyclonic flow and heavy rainfall are found around an IMD during the maximum phase. The IMD case in the minimum phase (July 22–24, 1991) showed a weaker circulation and less-organized rainfall (Fig. 7b). Two days after its mature phase, the IMD rainfall over India was reduced to about one-fourth of its maximum value and dissipated within another day.

The comparison of the IMD water budget between the maximum and the minimum phases of the 10–20 d monsoon mode (Fig. 5c) clearly reveals that the hydrological processes of the IMD are also affected by the 10–20 d monsoon mode through changes of convergence of water vapor flux. However, due to the weak intensity of the divergent circulation associated with the 10–20 d monsoon mode, the water vapor budget difference between the maximum and minimum phases is smaller (about 15%) in Fig. 7c than that between active and break phases (about 40%) shown in Fig. 6c.

6. Concluding remarks

Over a half of the Indian summer monsoon rainfall is produced by the IMD (e.g. Krishnamurti, 1979; Saha et al., 1981), although Mooley (1973) obtained an estimation of much smaller contribution. Unlike other tropical storms (e.g. typhoon or hurricane) which exist for longer periods over the ocean, a significant part of the IMD lifetime is located over the Indian subcontinent after its genesis over the head of the Bay of Bengal. Therefore, it is likely that the moisture source of the IMD is primarily supplied by convergence of water vapor flux, instead of evaporation. Convergence of water vapor flux is well coupled with the atmospheric lower-tropospheric divergent circulation. It was hypothesized that any change of this circulation by the 30–60 and 10–20 d monsoon modes might result in the change of convergence of water vapor flux, i.e. the moisture supply of the IMD, which induces the fluctuation of hydrological processes and the water budget of the IMD. This hypothesis was tested by our answers to the following two questions.

(i) What is the IMD contribution to the total monsoon rainfall? This contribution may be estimated from the composite water vapor budget of IMDs. Typically, six monsoon depressions (e.g. Chen and Weng, 1999) develop every monsoon season over the Bay of Bengal. It was shown by the composite analysis that an IMD could stay about 3–4 d (from day 1 to day 4) over the

Indian subcontinent with rainfall over 250 mm d^{-1}. A simple estimation of the total rainfall by IMDs (3–4 d × 25 mm d^{-1} × 6 is equivalent to about 45–55% of the total monsoon rainfall (92 d $season^{-1}$ × 12 mm d^{-1} = 1104 mm $season^{-1}$) over the computational domain (75°E–90°E, 15°N–27°N). This value is much higher than that estimated by Mooley (1973) due to difference in the analysis methods employed by both studies. Mooley (1973) used only six stations along the eastern coast of India to estimate the IMD contribution to the total rainfall over these stations, while the current study applied composite analysis using rainfall of GPCP, TRMM and GPI to estimate the contribution by the IMD to the total monsoon rainfall. About half of the total rainfall over the eastern coast of India is generated by the monsoon depressions.

(ii) How is the IMD water vapor budget modulated by the 30–60 and 10–20 d monsoon modes? The life cycle of the Indian summer monsoon (onset–break–revival–withdrawal) is formed by two intraseasonal modes. As the Indian monsoon undergoes its life cycle, convergence of the water vapor flux over India fluctuates in a coherent way. In other words, during active and minimum (break and minimum) phases, rainfall and convergence of the water vapor flux are enhanced (suppressed) over the Indian subcontinent (Figs. 3 and 5b). As we discussed earlier, the major water vapor source to an IMD is supplied through convergence of water vapor flux (≈60% shown in Fig. 5b). Because this basic hydrological process is needed to maintain the hydrological cycle of the IMD, its water vapor budget and hydrological processes are modulated by the two intraseasonal modes through their divergent circulations (Figs. 5–7). The IMD hydrological cycle is intensified (weakened) by the convergence (divergence) of water vapor flux associated with two intraseasonal modes during active/maximum (break/minimum) monsoons. On the other hand, it is revealed from the comparison between the IMD hydrological cycle during the two extreme phases of the 10–20 d mode that this intraseasonal monsoon mode exerts less effect than the 30–60 d mode.

In addition, to answer this question, another important feature of the IMD was revealed from the IMD hydrological processes. It was suggested by Saha and Chang (1983) that a cross-IMD asymmetric circulation was maintained by thermal advection: an upward branch west of the IMD center by warm advection and a downward branch of this center by cold advection. However, the thermal advection requires a baroclinic structure of the IMD. As shown by previous studies (e.g. Godbole, 1977; Chen and Yoon, 2000), the IMD does not exhibit a vertically westward tilt. Based on the heat budget analysis of a FGGE-MONEX depression, Saha and Saha (1988) suggested that the IMD asymmetric circulation should be maintained by the latent heat released from rainfall over this depression's west–south-west sector. It was indicated by hydrological processes of IMDs shown in Figs. 4, 6 and 7. that this asymmetric circulation was maintained by the east–west differential heating maintained by rainfall located over west/south-west of an IMD. The spatial relationship between the east–west asymmetric circulation and the IMD is opposite to the mid-latitude synoptic disturbance. This difference implies that there are differences in their dynamics which deserves further research.

7. Acknowledgments

This work was supported by a NASA Earth System Science Fellowship, the National Science Foundation Grant ATM-0434798, and the NASA Grant NAG512428. Editing assistance by Mr Dave Flory and typing support by Mr Simon Wang are highly appreciated. The GPI data were provided by Dr Joel Susskind at the Goddard Space Flight Center, NASA. Comments offered by two reviewers were helpful in improving the presentation in this paper.

References

Cadet, D. L. and Greco, S. 1987. Water vapor transport over the Indian Ocean during the 1979 summer monsoon. Part I: water vapor fluxes. *Mon. Wea. Rev.* **115**, 653–663.

Chen, T-C. 1985. Global water vapor flux and maintenance during FGGE. *Mon. Wea. Rev.* **113**, 1801–1819.

Chen, T-C. and Chen, J-M. 1993. The 10–20 day mode of the 1979 Indian monsoons: Its relation with the time variation of monsoon rainfall. *Mon. Wea. Rev.* **121**, 2465–2482.

Chen, T-C. and Weng, S-P. 1999. Interannual and intraseasonal variations in monsoon depressions and their westward-propagating predecessors. *Mon. Wea. Rev.* **127**, 1005–1020.

Chen, T-C. and Yen, M-C. 1986. The 40–50 day oscillation of the low-level monsoon circulation over the Indian Ocean. *Mon. Wea. Rev.* **114**, 2550–2570.

Chen, T-C. and Yoon, J-H. 2000. Some remarks on the westward propagation of the Monsoon depression. *Tellus* **52A**, 487–499.

Chen, T-C., Tzeng, R-Y. and Yen, M-C. 1988. Development and life cycle of the Indian monsoon: Effect of the 30–60 day oscillation. *Mon. Wea. Rev.* **116**, 2183–2199.

Chen, T-C., Yen, M-C. and Schubert, S. 1996. Hydrologic processes associated with cyclone systems over the United States. *Bull. Am. Meteorol. Soc.* **77**, 1559–1507.

Chen, T-C., Yoon, J-H. and Wang, S-Y. 2005. Westward propagation of the Indian monsoon depression. *Tellus* **57A**, 758–769.

Cressman, G. P. 1959. An operational objective analysis system. *Mon. Wea. Rev.* **87**, 367–374

Daggupaty, S. M. and Sikka, D. R. 1977. On the vorticity budget and vertical velocity distribution associated with the life cycle of a monsoon depression. *J. Atmos. Sci.* **34**, 773–792.

Gibson, J. K., Kallberg, S., Hernandez, A., Uppala, S., Nomura, A. and co-authors. 1997. *ERA Description*, ECMWF Reanalysis Project Report Series Vol. 1, ECMWF, Shinfield Park, Reading, RG2 9AX, UK, 72 pp.

Godbole, R. V. 1977. The composite structure of the monsoon depression. *Tellus* **29**, 25–40.

Goswami, B. N., Krishnamurthi, V. and Annamalai, H. 1999. A broad-scale circulation index for the interannual variability of the Indian summer monsoon. *Q. J. R. Meteorol. Soc.* **125**, 611–633.

Huffman, G. J., Adler, R. F., Arkin, P., Chang, A., Ferraro, R. and co-authors. 1997. The Global Precipitation Climatology Project (GPCP) Combined Precipitation Data Set. *Bull. Am. Meteorol. Soc.* **78**, 5–20.

Krishnamurti, T.-N. 1979. Tropical Meteorology. In: *Compendium of Meteorology II* (ed. A. Wiin-Nielsen), WMO-No. 364, World Meteorological Organization, 428 pp.

Krishnamurti, T.-N. and Ardanuy, D. 1980. The 10 to 20 day westward propagating mode and "Breaks in the monsoons". *Tellus* **32**, 15–26.

Krishnamurti, T.-N. and Bhalme, H. H. 1976. Oscillations of a monsoon system. Part I: observational aspects. *J. Atmos. Sci.* **33**, 1937–1954.

Krishnamurti, T.-N. and Subrahmanayam, D. 1982. The 30–50 day mode at 850 mb during MONEX. *J. Atmos. Sci.* **39**, 2088–2095.

Krishnamurti, T.-N., Kanamitsu, M., Godbole, R., Chang, C-B., Carr, F. and co-authors. 1975. Study of a monsoon depression (I): synoptic structure. *J. Meteorol. Soc. Japan* **53**, 227–239.

Krishnamurti, T.-N., Kanamitsu, M., Godbole, R., Chang, C-B., Carr, F. and Chow, J. H. 1976. Study of a monsoon depression (II): dynamical structure. *J. Meteorol. Soc. Japan* **54**, 208–226.

Krishnamurti, T.-N., Molinari, J., Pan, H. and Wang, V. 1977. Downstream amplification and formation on monsoon disturbances. *Mon. Wea. Rev.* **105**, 1281–1297.

Krishnamurti, T.-N., Jayakumar, P. K., Sheng, J., Sugri, N. and Kumar, A. 1984. Divergent circulations on the 30 to 50 day time-scale. *J. Atmos. Sci.* **42**, 364–375.

Mooley, D. A. 1973. Some aspects of Indian monsoon depressions and the associated rainfall. *Mon. Wea. Rev.* **101**, 271–280.

Murakami, M. 1976. Analysis of summer monsoon fluctuations over India. *J. Meteorol. Soc. Japan* **54**, 15–31.

Murakami, M. 1979. Large-scale aspects of deep convective activity over the GATE area. *Mon. Wea. Rev.* **107**, 997–1013.

Murakami, T., Nakazawa, T. and He, J. 1984. On the 40–50 day oscillations during the 1979 Northern Hemisphere summer. Part II: heat and moisture budget. *J. Meteorol. Soc. Japan* **62**, 469–484.

Nitta, T. and Masuda, K. 1981. Observational study of a monsoon depression developed over the Bay of Bengal during the summer MONEX. *J. Meteorol. Soc. Japan* **59**, 672–682.

Ramage, C. S. 1971. *Monsoon Meteorology*. Academic Press, New York, 296 pp.

Riehl, H. 1954. *Tropical Metoerology*. McGraw-Hill, New York.

Saha, K. and Bavardeckar, S. N. 1976. Moisture flux across the west of India and rainfall during the southwest monsoon. *Tellus* **38**, 370–379.

Saha, K. and Chang, C-P. 1983. The baroclinic processes of monsoon depressions. *Mon. Wea. Rev.* **111**, 1506–1514.

Saha, K. and Saha, S. 1988. Thermal budget of a monsoon depression in the Bay of Bengal during FGGE-MONEX 1979. *Mon. Wea. Rev.* **116**, 242–254.

Saha, K., Sanders, F. and Shukla, J. 1981. Westward propagating predecessors of monsoon depressions. *Mon. Wea. Rev.* **109**, 330–343.

Sikka, D. R. 1977. Some aspects of the life history, structure and movement of monsoon depressions. *Pure Appl. Geophys.* **115**, 1501–1529.

Simpson, J. S., Kummerow, C., Tao, W-K. and Adler, R. F. 1996. On the Tropical Rainfall Measuring Mission (TRMM). *Meteorol. Atmos. Phys.* **60**, 19–36.

Stano, G., Krishnamurti, T. N., Vijaya Kumar, T. S. V. and Chakraborty, A. 2002. Hydrometeor structure of a composite monsoon depression using TRMM radar. *Tellus* **54A**, 370–381.

Susskind, J., Piraino, P., Rokke, L., Iredell, L. and Mehta, A. 1997. Characteristics of the TOVS Pathfinder Path A data sets. *Bull. Am. Meteorol. Soc.* **78**, 1449–1472.